

CORROSION MITIGATION WITH pH STABILISATION IN SLIGHTLY SOUR GAS/CONDENSATE PIPELINES

Jon Kvarekval and Arne Dugstad
Institute for Energy Technology
PO Box 40
N-2027 Kjeller
NORWAY

ABSTRACT

An experimental study focused on the applicability of pH-stabilisation for corrosion control in sour environments with hydrate preventer has been carried out, consisting of flow loop experiments with 50 % diethylene glycol, 0.02 bar H₂S and 2 bar CO₂. pH values in the range of 6.0-7.0 were investigated. The experiments were run at flow velocities between 1 and 3 m/s and temperatures of 20, 60 and 120°C. It has been shown that pH-stabilisation at a target pH of 7.0 seems to give sufficient corrosion protection under these conditions. The steady state uniform corrosion rates were 10 times less at pH 7 (0.01 mm/y) than at pH 6.5 (0.1-0.2 mm/y). While a few cases of pitting and edge corrosion were found on the specimens exposed at pH 6.5, no localised attacks occurred at pH 7.0. The intensity of corrosion attacks was similar for the three types of carbon steel (St52, X65 and Cr0.5) used in the tests. The findings have contributed to increased confidence in pH stabilisation as a viable corrosion control method for natural gas pipelines with low H₂S levels.

Keywords: Corrosion, carbon steel, pitting, CO₂, H₂S, iron sulfide, pH stabilisation.

INTRODUCTION

An increasing number of wet gas carbon steel pipelines use glycol for hydrate prevention and the pH-stabilisation technique for corrosion control¹. The basis of pH-stabilisation is addition of alkaline chemicals (e.g. NaOH or methyldiethanolamine, MDEA) to corrosive media in order to increase pH of the glycol/water mixture and thus improve the protective properties of the corrosion films. The pH-stabilisation technique has so far been applied mainly in sweet pipelines, but it has recently also been used or selected for H₂S-containing offshore fields in the Persian Gulf, the North Sea and Oceania.

A three year research program was run from 1993 to 1996 - Kjeller pH-stabilisation Project phase I - together with several oil companies to determine the optimum treatment methods in CO₂ environments with respect to chemicals, pH, temperature etc.^{2,3} The experiences from sweet fields so far have been very good. Corrosion rates far below 0.1 mm/year have been reported for all the systems, even when the CO₂ partial pressure was higher than 10 bar. The effect of H₂S on protective film formation has been studied in the Kjeller pH stabilisation Project phase II (1999-2001)⁴ and the ongoing Kjeller Sour Gas Project (2002-2006). These projects focused on the feasibility of pH-stabilisation technique in wet gas/condensate pipelines with up to 5 bar total pressure of CO₂ and H₂S. Pitting corrosion turned out to be a larger problem in glycol solutions exposed to H₂S partial pressures higher than 0.1 bar than in CO₂ solutions at similar pH⁵. At lower H₂S partial pressures, however, the results were more uplifting. A series of flow loop tests carried out at 0.02 bar H₂S and 2 bar CO₂ showed that pH stabilisation can be feasible in pipelines with low H₂S levels.

EXPERIMENTAL

Corrosion experiments was carried out in a flow loop designed for inhibitor testing, high temperature testing, experiments with H₂S, experiments under scaling conditions and experiments with oil/water wetting. All components in contact with the loop water are made in Hastelloy C-276*. A flow diagram of the loop is shown in Figure 1. The loop is built with a main circuit with 25 mm inner diameter. Maximum pressure and temperature are 50 bar and 150°C. A centrifugal pump with canned motor is used to circulate the water at flow velocities up to 10 m/s.

The loop has three horizontal test sections, which can be bypassed and operated independently. One of the test sections can be periodically exposed to stagnant, dry or oil wet conditions in order to study variation in operational parameters. The water phase can be continuously renewed. Several autoclaves where corrosion products or scale can be precipitated out or dissolved are connected to the loop. The sequence of the operational conditions can be programmed and run automatically. The test sections can accommodate both flat and flush mounted tubular specimens. The test specimens consisted of flat steel coupons mounted in a row along the diameter of the flow channel as illustrated in Figure 2.

Chemicals

The test solutions were made from distilled water with 0.1 % NaCl, with the addition of 50 weight-% diethylene glycol (DEG) in the experiments with hydrate preventer. pH adjustments were made with Puriss grade sodium hydroxide (NaOH). NaOH reacts instantly with dissolved CO₂ and H₂S

* Trademark of Haynes International Ltd.

to form bicarbonate (HCO_3^-) and bisulfide (HS^-) ions respectively. The test solutions were pressurised with CO_2 and H_2S gas in order to attain the required concentrations. The CO_2 gas used was grade 4.0 or better, while the H_2S gas was grade 2.8. None of the gases contained significant amounts of contaminants that would affect the experiments, e.g. oxygen.

The content of CO_2 , H_2S , Fe^{2+} and the pH of the test solutions were measured regularly and adjusted if necessary. The CO_2 content in the test solutions was determined by water analysis based on precipitation of BaCO_3 when loop water is fed into a barium hydroxide solution. The H_2S concentration was determined by titration of loop water samples against an ion selective electrode ($\text{Ag}^+/\text{S}^{2-}$). pH was measured using two pH combination electrodes mounted in small bypass lines. The pH electrodes were calibrated in aqueous buffers with pH 7 and 4 prior to use. When using the electrodes in glycol solutions the measured pH may deviate somewhat from the real pH. In solutions with 50 % monoethylene glycol (MEG) the measured pH is about 0.2 pH units lower than the real pH⁶. Correction factors for DEG solutions are not available, although similar values as in MEG solutions could be expected.

Test coupons

Small variations in microstructure and chemical composition can influence the corrosion rate and the type of attack considerably, and therefore three types of carbon steel were included in the study: St52, regular X65 steel and an X65 steel with chromium addition (0.5% Cr). The elemental composition of the steels is shown in Table 1.

For the loop experiments 3 mm thick steel coupons with dimensions 25 mm x 25 mm were used (Some of the 0.5% Cr steel coupons were 17 mm x 25 mm). The coupons were machined from pipeline steel samples. Both sides of the specimens were exposed, giving a total exposed surface area of about 12 cm² per coupon.

Prior to immersion, all specimens were ground with mesh 1000 SiC abrasive paper, cleansed in an ultrasonic acetone bath, then flushed with ethanol and acetone. The specimens were blow dried with a hot air gun.

Corrosion rate measurements

The general corrosion rate was determined by weight loss measurements and linear polarisation resistance (LPR). A common three-electrode set-up was used for LPR measurements. Adjacent test coupons were used as reference electrodes, while Hastelloy C strips were used as counter electrodes. The LPR measurements were performed using Gamry PC3/750 potentiostats with multiplexers. Additional specimens without electrochemical connections were included in the Hastelloy loop experiments, and the average corrosion rates of these specimens were determined by weight loss.

LPR measurements are performed by using a slow potential sweep (0.1 mV/s) from -5 mV to +5 mV vs. the free corrosion potential. The polarisation resistance R_p is determined from the slope of the obtained current/potential curve and the current density is given as:

$$i_{corr} = \frac{B}{R_p A}$$

where B is the LPR constant and A is the specimen area. The B values were determined from weight loss data, and were found to be in the range of 10-30 mV.

An optical microscope with a scaled focus knob was used for pit depth measurements. The depth of the localised attack (in μm) was directly obtained by shifting the focus from the general corrosion front or a non-corroded reference point to the bottom of the pit.

RESULTS

Results from flow loop corrosion experiments with simulated sour gas pipeline aqueous phase are presented here. All experiments were carried out with water/glycol mixtures to study the effect of chemical hydrate prevention on corrosion control with pH stabilisation. The test conditions and some key results are given in Table 2.

Flow loop tests were carried out at temperatures of 20, 60 and 120°C, all with 50 wt-% DEG, 0.02 bar H₂S, 2 bar CO₂, 0.1 wt-% NaCl and flow velocities 1-3 m/s. pH values in the range of 6.0-7.0 were attained by addition of NaOH. Test coupons were made of three types of carbon steel; St52, X65 and 0.5% Cr. A total of about 100 test coupons were exposed to the above conditions in this study. A selection of representative results is presented below.

Tests at 20°C and pH 6.5

Figure 3 depicts LPR corrosion rate vs. time curves for test specimens exposed at a flow velocity of 3 m/s. The LPR corrosion rates measured on coupons exposed at flow velocities of 1 and 2 m/s were similar to those obtained at 3 m/s. The mean corrosion rates on all steels were less than 0.1 mm/y during the entire test period. Low initial corrosion rates indicate fast-forming protective corrosion films, consisting of thin layers of iron sulfide (mackinawite). The surface appearances of stripped test coupons are shown in Figure 4. Examination in optical microscope showed that small pits had been formed. Maximum local attack depth was 30 μm , corresponding to a penetration rate of 0.3 mm/y.

Tests at 60°C and pH 6.5-7.0

The tests at 60°C were carried out with a flow velocity of 2 m/s in all test racks. Figures 5-7 depict LPR corrosion rates at pH 6.5 and 7.0. Initial corrosion rates at pH 6.5 were typically 0.2-0.4 mm/y (Figure 5). In 5-10 days the corrosion rates decreased to 50 % of the initial values, after which a very slow increase was observed. Figure 6 shows effect of a pH increase from 6.5 to 7.0 on corrosion rates. The pH increase caused a marked drop in the LPR corrosion rates, which stabilised around 0.02 mm/y at pH 7. Even lower corrosion rates, less than 0.01 mm/y were observed when fresh coupons were exposed at pH 7, without “precorrosion” at pH 6.5 (Figure 7). Although the corrosion rates increased slowly with time throughout the 6-week exposure period, the typical upper limit of acceptable corrosion (0.1 mm/y) was not approached.

Surface appearances of stripped coupons exposed for 44 days at pH 6.5 are shown in Figure 8. Local corrosion has taken place on the edges of the coupons. A few shallow pits with depths up to 45 μm were found. SEM pictures of cross-sectioned test coupons (both X65) with intact corrosion film are shown in Figure 9. The corrosion films were 5-10 μm thick and covered most of the exposed surfaces. Areas without adherent corrosion films did not appear to have corroded faster than film-covered areas, i.e. no mesa corrosion occurred. Some edge corrosion attacks with up to 300 μm depth took place on one of the X65 coupons exposed for 69 days at pH 6.5 (Figure 5). The depth of the uniform attack on this coupon was 25-35 μm . No localised corrosion attacks were found on the coupons exposed at pH 7.0.

Tests at 120°C and pH 6.0-6.5

Figure 10 shows LPR corrosion rate vs. time curves for test specimens exposed at 3 m/s. Curves for 1 and 2 m/s were similar. Variations in pH during the experiment are also indicated in the chart. The first 14 days of the experiment were run at pH 6.0, after which the pH was increased to 6.5. Initial corrosion rates were about 1 mm/y, but dropped significantly during the first two days. After 1 week the corrosion rates were less than 0.1 mm/y on all specimens. When pH was increased from 6 to 6.5 after 14 days the corrosion rates decreased even more. The reduction in corrosion rates during the first few days of the experiment indicate that protective corrosion films were formed in this period.

The corrosion films on the Cr0.5 specimens were flaky and easily removed, while the films on the St52 and X65 specimens were dense, adherent and difficult to dissolve. A stripping procedure of more than 30 minutes immersion in inhibited HCl followed by 1 hr ultrasonic cleaning was required to completely remove the corrosion films.

The weights of the exposed specimens with corrosion films were higher than coupon weights before the experiment. The ratio of metal weight loss to film weight was about 0.7 for all specimens, while the theoretical weight-to-weight ratio of equimolar amounts of iron (Fe) and iron sulfide (FeS) is 0.64. Thus, assuming that only FeS was formed, it is clear that more than 90 % of the dissolved steel precipitated and remained on the specimen surfaces.

Figure 11 shows surface appearance of the test specimens after stripping. Pitted areas can easily be seen. The maximum detected pit depth corresponded to a local corrosion rate of 0.63 mm/y. Cross-sectioning and SEM examinations of specimens with film showed that the FeS had accumulated above the pits, see Figure 12. In general the surfaces were covered by FeS corrosion films less than 10 μm thick.

The corrosion films formed at 120°C were denser and more adherent than those formed at lower temperatures, and seemed more protective. X-ray diffraction spectra for coupons exposed at 60°C and 120°C are given in Figures 13 and 14 respectively. Despite the high background noise typical for iron compounds, the mackinawite *d* lines (5.03 kV, 2.31 kV, 2.97 kV, ranked by descending intensity) can be identified on both spectra. In addition, lines for pyrrhotite (2.057 kV, 2.635 kV, 2.966 kV) are present in the spectrum for 120°C (Figure 14), indicating that the corrosion films formed at this temperature consisted of a mixture of mackinawite and pyrrhotite. Pyrrhotite has been detected in corrosion films formed at temperatures higher than 80°C⁷, and was not detected in corrosion films produced at 20-60°C in this study.

DISCUSSION

Hydrate preventers have been reported to have an inhibiting effect in sweet systems with and without pH stabilisation, but the amount of published research work on sour systems with hydrate preventers is small. Results published at CORROSION/2005⁵ indicate that the maximum local penetration (pitting) rates can be very high at around 1 bar H₂S. Furthermore, it was demonstrated that temperature may be a crucial parameter for protective FeS film formation.

In the experiments carried out with low H₂S levels (20 mbar) most of the experimental work was focused on a target pH of 6.5. At this pH value the steady state LPR corrosion rates were less than 0.1 mm/y on almost all coupons exposed. However, localised corrosion rates were up to 0.4 mm/y at 60°C. The results obtained at 20 and 60°C did not clearly indicate that the pit growth slowed down with time, but the results of supplemental glass cell experiments, previously published at CORROSION/2004⁸, showed that the pits formed under similar conditions actually became inactive after a period of growth.

While pitting corrosion was observed at 60°C and pH 6.5, no localised corrosion occurred and the general corrosion rates were around 0.01 mm/y and during 40 days exposure at pH 7.0. Furthermore, test coupons exposed at both pH 6.5 and 7.0 experienced a significant drop in corrosion rate when the pH was increased. The corrosion films consisted of 5-10 µm thick iron sulfide films. Based on these observations pH-stabilisation at a target pH of 7.0 seems to give sufficient corrosion protection at 0.02 bar H₂S, 2 bar CO₂, 20-120°C and moderate flowing conditions.

The combined mackinawite/pyrrhotite corrosion films formed at 120°C seemed more protective than the mackinawite films formed at 20 and 60°C, and it is likely that the pits formed during the initial period with high corrosion rates at 120°C became less active with time. The very good adherence of the corrosion product film experienced during stripping also supports this assumption. In general, the severity of the pitting attacks did not appear to depend on flow velocities in the range 1-3 m/s.

CONCLUSIONS

A corrosion study focused on the applicability of pH-stabilisation in sour environments with hydrate preventer has been carried out, consisting of flow loop experiments with 50 % diethylene glycol, 0.02 bar H₂S and 2 bar CO₂. Different pH values in the range of 6.0-7.0 were applied. The experiments were run at flow velocities up to 3 m/s and temperatures 20-120°C.

pH-stabilisation at a target pH of 7.0 seems to give sufficient corrosion protection under mildly sour conditions with 0.02 bar H₂S and 2 bar CO₂ at temperatures between 20 and 120°C. The steady state uniform corrosion rates were 10 times less at pH 7 (0.01 mm/y) than at pH 6.5 (0.1-0.2 mm/y). While a few cases of pitting and edge corrosion were found on the specimens exposed at pH 6.5, no localised attacks occurred at pH 7.0. Considering the results from the loop tests as well as supplemental results of planned-interval glass cell experiments⁸, it appears that the pits formed at pH 6.5 stopped growing after a while, thus being acceptable from the aspect of long-term corrosion control. The intensity of corrosion attacks was similar for the three types of carbon steel (St52, X65 and Cr0.5) used in the tests.

The presence of hydrate preventer (MEG/DEG) seems to complicate the use of pH-stabilisation in H₂S/CO₂ systems, making the steel more susceptible to pitting than in purely aqueous solutions. This is a problem that must be resolved or controlled in order to apply pH-stabilisation in sour gas pipelines. The present findings show that pH stabilisation may be feasible for corrosion control at H₂S partial pressures up to 0.02 bar, but the development and possible consequences of long-term localised corrosion attack requires further studies. Put in a wider perspective, however, the main problems associated with application of pH stabilisation are rarely related to corrosion protection alone, but also other process problems such as scaling in the pipelines due to formation water carryover, suspension of solid fines and particles causing filter clogging, and salt precipitation in MEG-regeneration boilers.

ACKNOWLEDGEMENT

The study was carried out as part of a joint industry project, Kjeller pH-stabilisation Project II. The authors wish to acknowledge the participants and sponsors of the project for kind permission to publish the results of this study.

REFERENCES

1. A. Dugstad, R. Nyborg, M. Seiersten, "Flow Assurance in pH Stabilised Wet Gas Pipelines", CORROSION/2003, Paper no. 03314, Nace International, Houston, TX, 2003.
2. A. Dugstad and P.-E. Drønen, "Efficient Corrosion Control of Gas Condensate Pipelines by pH-Stabilisation", CORROSION/99, Paper No. 20, Nace International, Houston, TX, 1999.
3. Arne Dugstad and Liv Lunde: Corrosion Mitigation by pH-stabilisation - Applications and Limitations. 9th Middle East Corrosion Conference, Bahrain, 12-14 February 2001. E.Gulbrandsen, J.-H.Morard, "Why Does Glycol Inhibit CO₂ Corrosion?", Paper no. 221, CORROSION/98, NACE International, TX, 1998.
4. J. Kvarekvål, M.Seiersten, A.Dugstad," Improved Corrosion Control in Wet Gas Pipelines", Kjeller pH-stabilisation Project II, Final report, IFE/KR/F-2001/136 (Confidential), 2001.
5. J. Kvarekvål, A. Dugstad, "Pitting Corrosion in CO₂/H₂S-containing Glycol Solutions under Flowing Conditions", Paper no. 05631, CORROSION/2005, NACE International, Houston, TX, 2005.
6. E.Gulbrandsen, J.-H.Morard, "Why Does Glycol Inhibit CO₂ Corrosion?", Paper no. 221, CORROSION/98, NACE International.
7. A.G. Wikjord, T.E. Rummery, F.E. Doern, D.G. Owen. "Corrosion and Deposition During the Exposure of Carbon Steel to Hydrogen Sulfide-Water Solutions". p. 651-671, Corrosion Science Vol. 20, 1980.

8. J. Kvarekvål, A. Dugstad, “Pitting Corrosion Mechanisms on Carbon Steel in Sour Glycol/Water Mixtures”, Paper no. 04737, CORROSION/2004, NACE International, Houston, TX, 2004.

TABLE 1
STEEL COMPOSITION AND MICROSTRUCTURE.

Steel	C	Si	Mn	S	P	Cr	Ni	V	Mo	Cu	Al	Micro-structure*
X-65	0.057	0.22	1.56	0.002	0.013	0.05	0.04	0.04	0.02	0.01	0.041	F + P
0.5% Cr	0.072	0.17	0.89	0.002	0.014	0.6	0.02	0.02	0.01	0.01	0.038	F + W
St52	0.12	0.17	1.62	0.011	0.016	0.03	0.04	0.014	0	0.02	0.029	F + P

*F - Ferrite, P - Pearlite, W - Widmanstättenferrite,

TABLE 2
EXPERIMENTAL CONDITIONS AND RESULTS FOR THE FLOW LOOP EXPERIMENTS

Temp. (°C)	pH	p_{CO_2} (bar)	p_{H_2S} (bar)	Flow (m/s)	Duration (days)	Final corr. rates (mm/y)	Max. local corr.rate ¹ (mm/y)
20	6.5	2.0	0.02	1, 2, 3	35	0.01-0.04	0.3
60	6.5	2.0	0.02	1,2,3	20-70	0.05-0.2	0.4 (1.5 ²)
60	7.0	2.0	0.02	2		0.01-0.02	-
120	6.0-6.5	2.0	0.02	1, 2, 3	30	0.01-0.02	0.6

1. Based on difference between uniform corrosion front and bottom of deepest pit.
2. Edge corrosion attack.

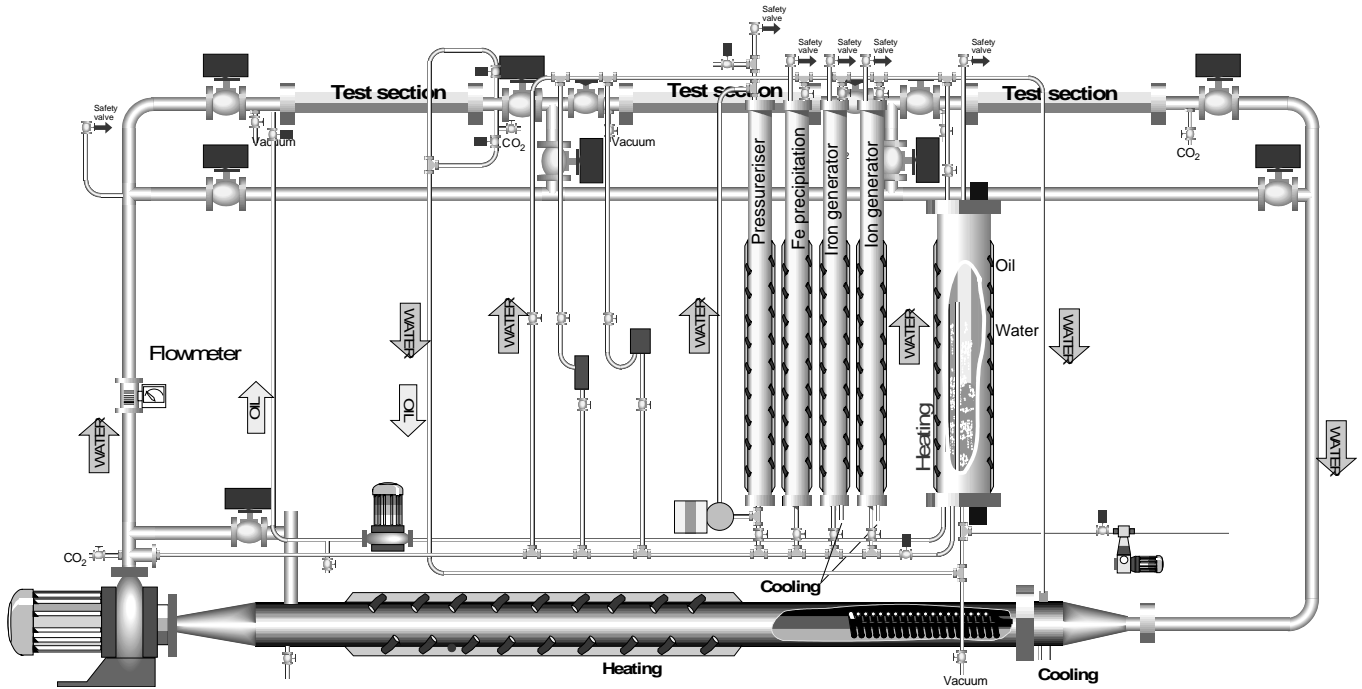


FIGURE 1 - Schematic illustration of the Hastelloy C corrosion testing loop.

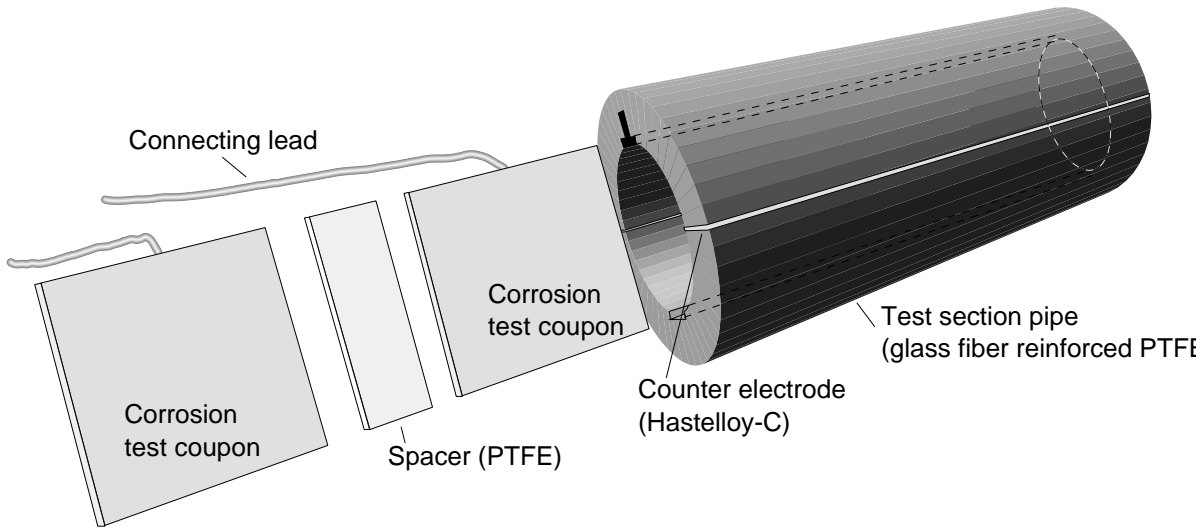


FIGURE 2 - The PTFE lining with specimen mounting in the tubular test rack.

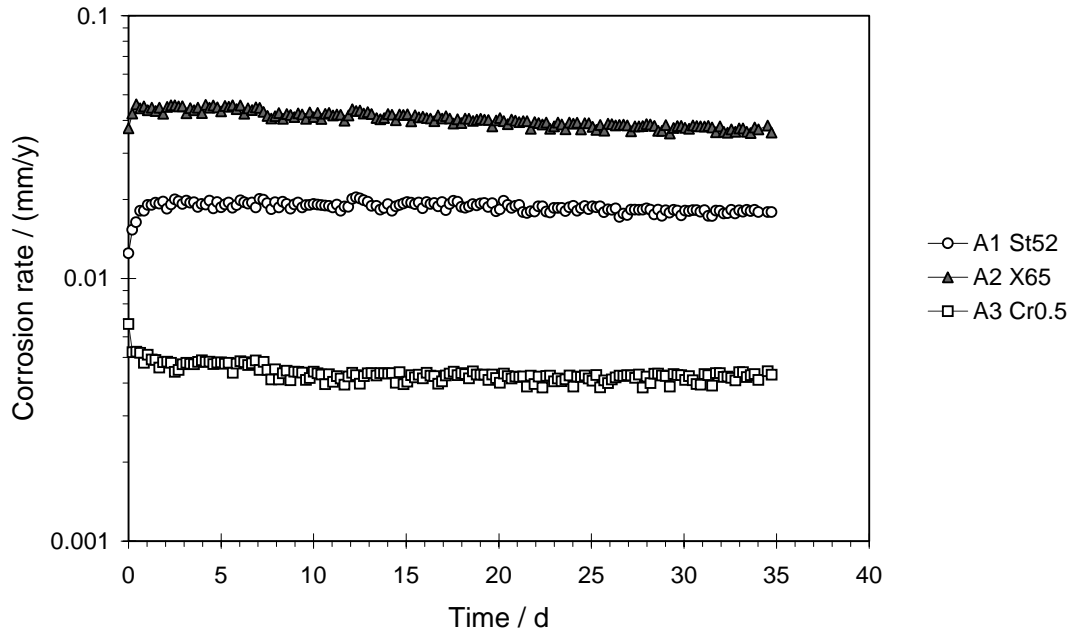


FIGURE 3 - Corrosion rates as a function of time, loop test 1
 Flow velocity 3 m/s. 50 % DEG, 20°C, 0.1 % NaCl, 2 bar CO₂,
 0.02 bar H₂S, fresh abraded specimens.

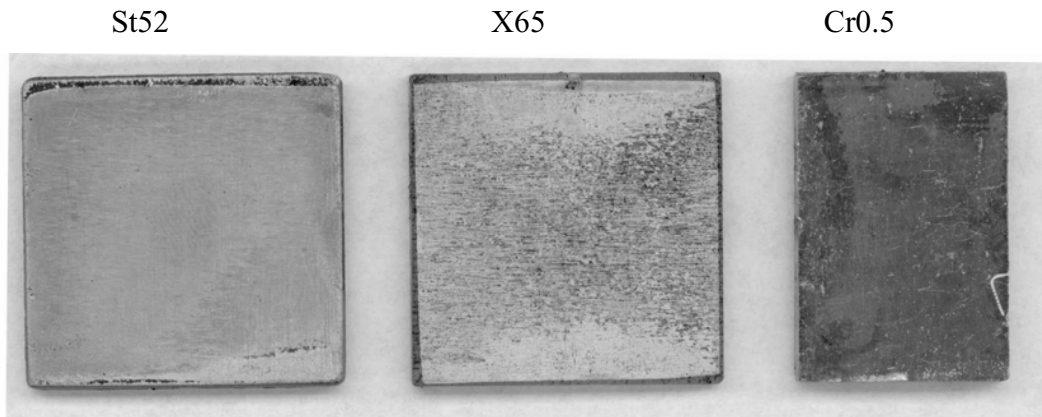


FIGURE 4 - Surface appearance of test specimens A1-3, B1-3 and C1-3, exp. L6, after stripping.

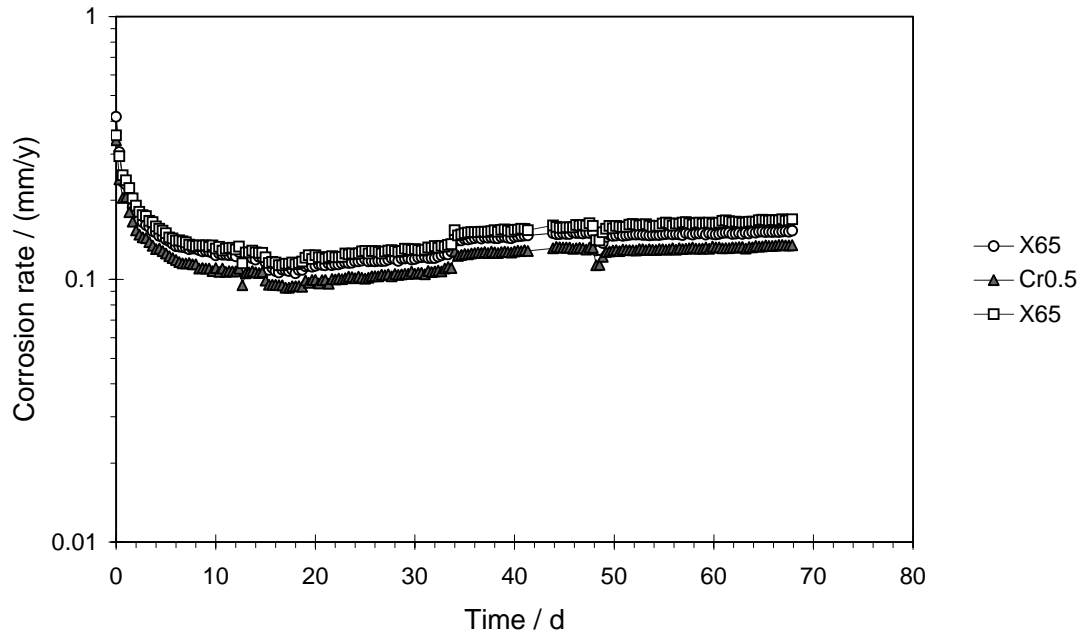


FIGURE 5 - Corrosion rates vs. time measured in the loop test at 60°C.
pH 6.5, 50% DEG, 2 bar CO₂, 20 mbar H₂S, flow velocity 2 m/s.

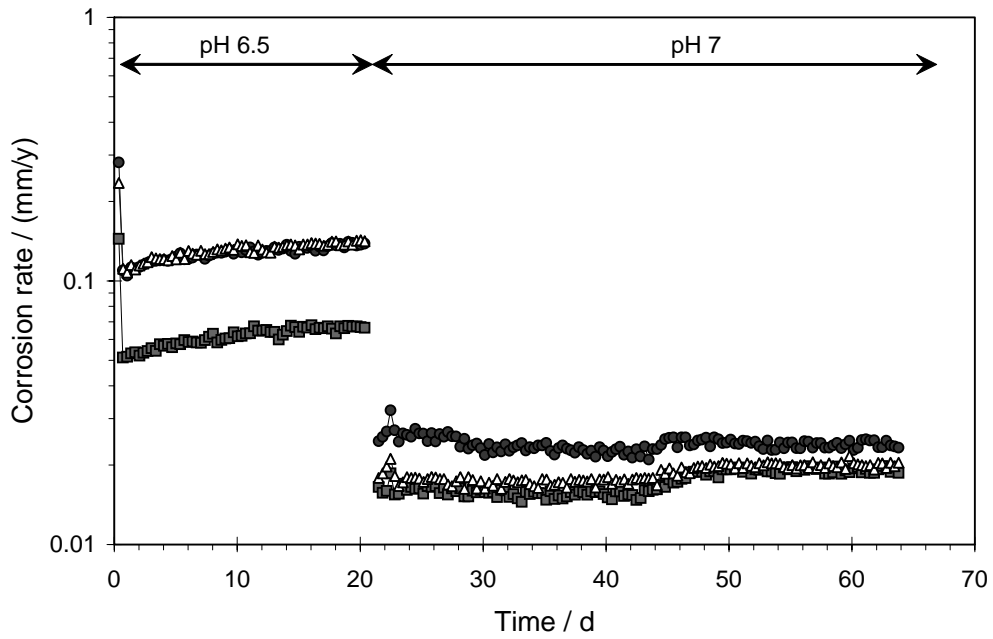


FIGURE 6 - Corrosion rates vs. time on X65 steel coupons exposed in the loop test at 60°C.
pH 6.5-7, 50% DEG, 2 bar CO₂, 20 mbar H₂S, flow velocity 2 m/s.

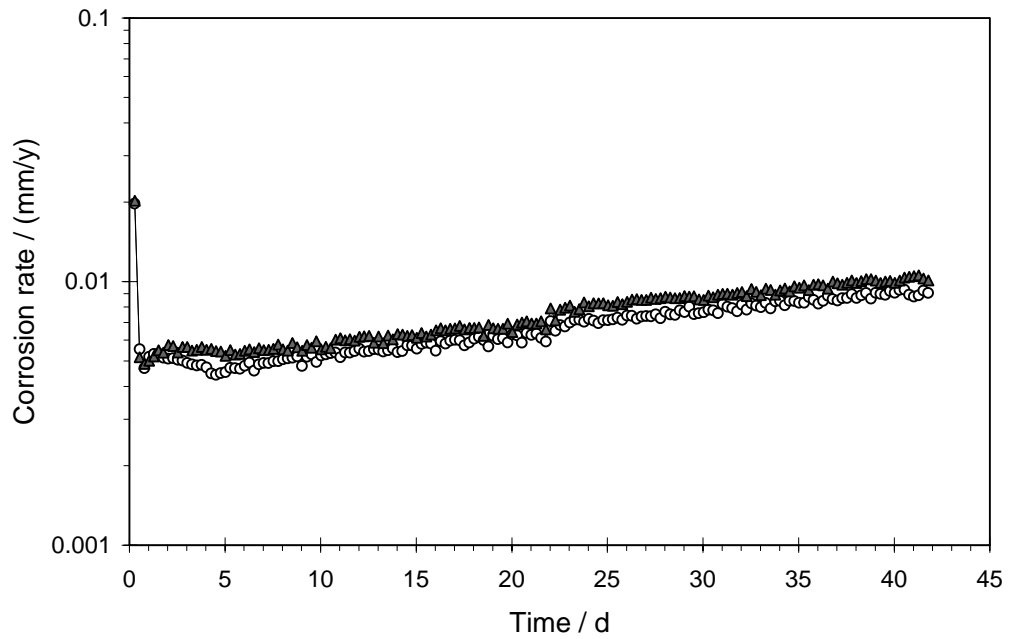


FIGURE 7 - LPR corrosion rates vs. time on X65 steel coupons exposed in the loop test at 60°C. pH 7, 50% DEG, 60°C, 1 bar CO₂, 20 mbar H₂S, flow velocity 2 m/s.

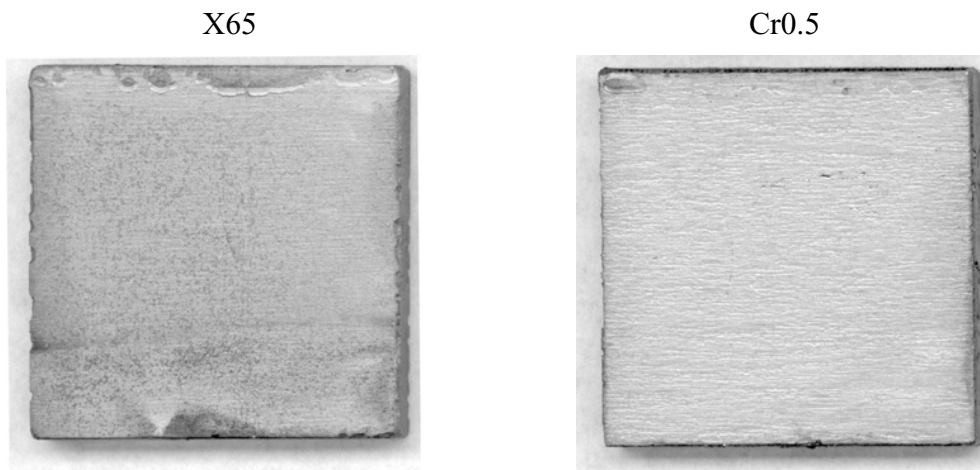


FIGURE 8 - Surface appearance of test coupons exposed for 44 days at 60°C and pH 6.5. 50% DEG, 2 bar CO₂, 20 mbar H₂S, flow velocity 2 m/s.

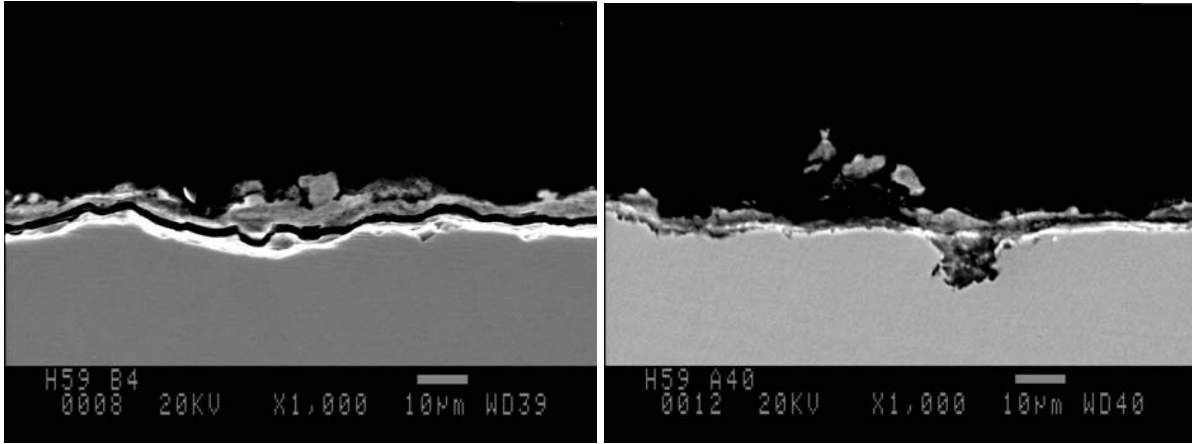


FIGURE 9 - SEM pictures of X65 specimens exposed at 60°C and pH 6.5.

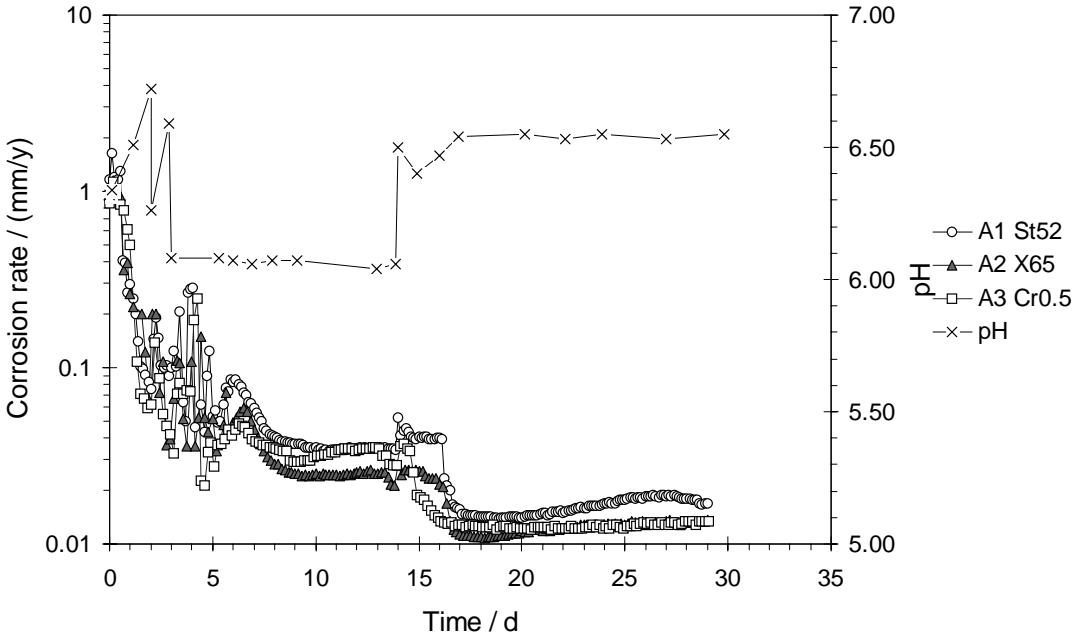


FIGURE 10 - LPR corrosion rates vs. time on X65 steel coupons exposed in the loop test at 120°C. pH 6.0-6.5, 50 % DEG, 60°C, 1 bar CO₂, 20 mbar H₂S, flow velocity 2 m/s.

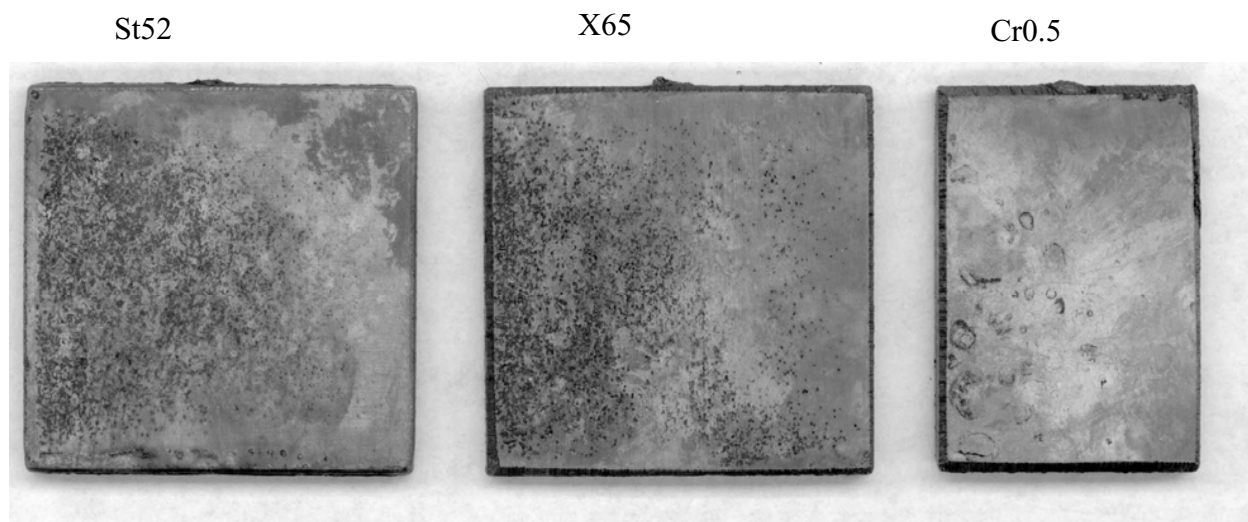


FIGURE 11 - Surface appearance of test coupons exposed at 120°C and 3 m/s flow velocity, after stripping

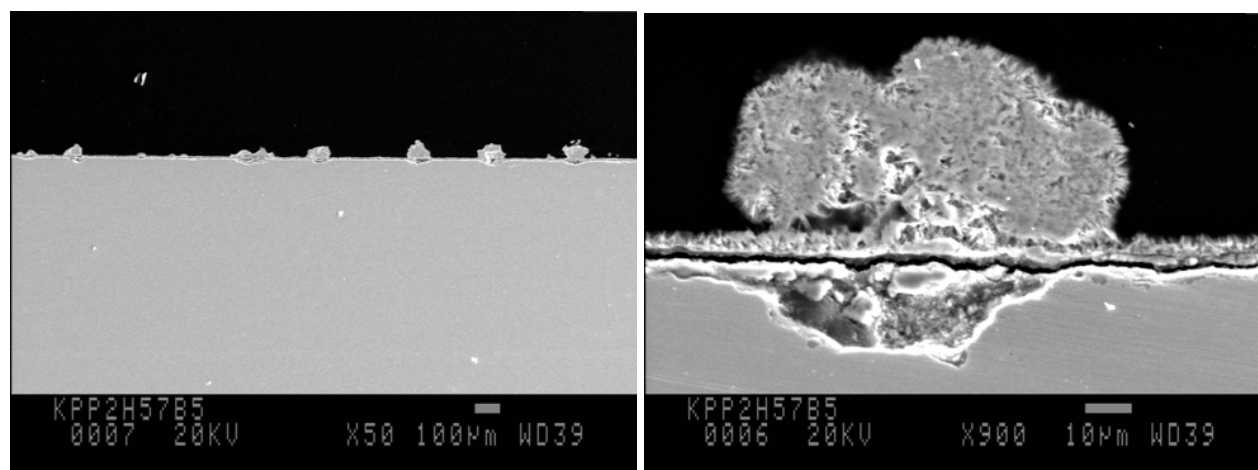


FIGURE 12 - SEM pictures (cross-section) of test coupon with corrosion film, exposed in the 120°C flow loop test. Accumulation of iron sulfides on top of small pits.

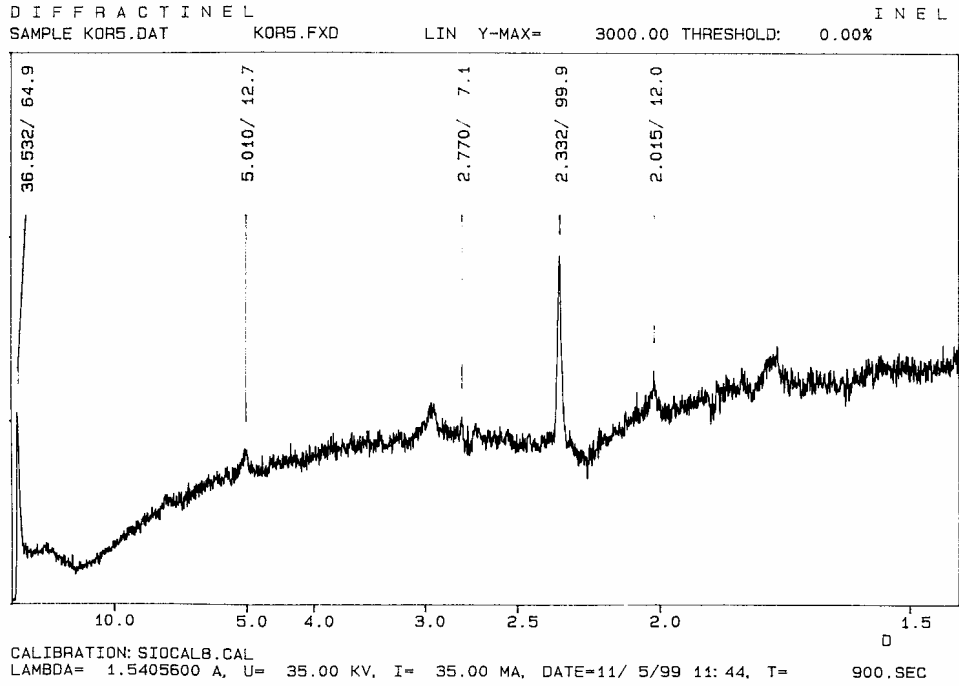


FIGURE 13 - XRD spectrum for corrosion product films from X65 steel coupons exposed in the 60°C loop test.

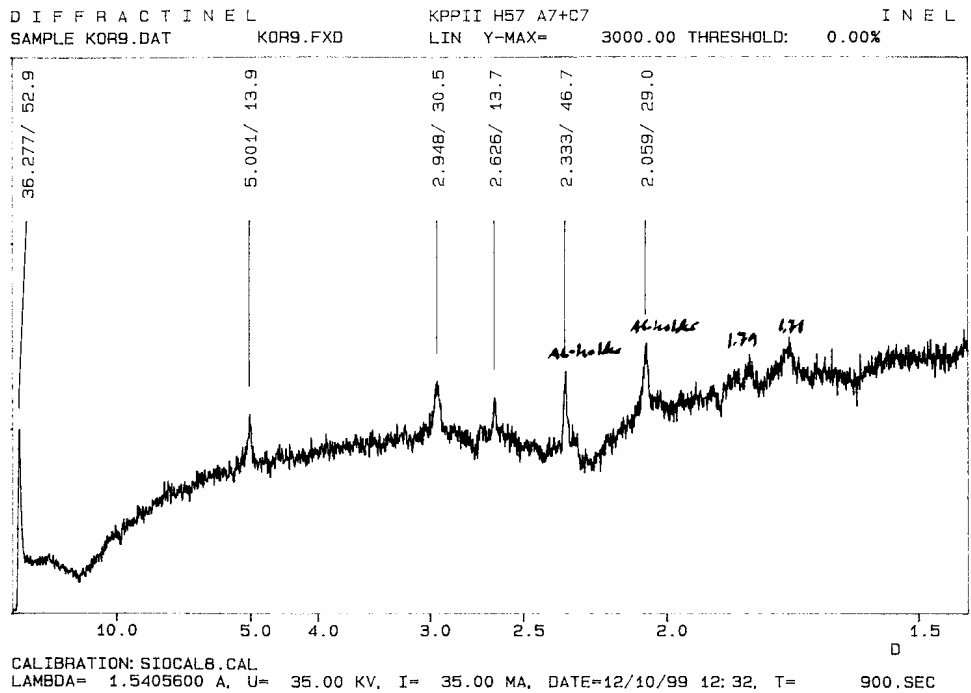


FIGURE 14 - XRD spectrum for corrosion product films from X65 steel coupons exposed in the 120°C loop test.